# Verification and Improvement of the Capability of ENSEMBLES to Predict the Winter Arctic Oscillation

Dapeng Zhang[1], Yanyan Huang[1], and Bo Sun[1]

[1]Collaborative Innovation Center on Forecast and Evaluation of Meteorological Disasters/Key Laboratory of Meteorological Disaster, Ministry of Education, Nanjing University of Information Science and Technology, Nanjing, China

November 22, 2022

## Abstract

The winter Arctic Oscillation (AO) is important for understanding the Northern Hemisphere climate variability and predictability. However, ENSEMBLES models produce inconsistent predictions when applied to the interannual variability of the 1962–2006 winter AO. In this study, the interannual increment of the winter AO index (DY_AOI) during 1962–2006 is first improved by a dynamical-statistical model with two predictors: the preceding autumn Arctic sea ice and the concurrent winter ENSEMBLES-predicted sea surface temperature over the North Pacific. Next, the improved final AOI is obtained by adding the improved DY_AOI to the preceding observed AOI. Because the interannual increment approach can amplify prediction signals and takes advantage from the previous observed AOI, this method shows promise for significantly improving the interannual variability prediction capabilities of the winter AO during 1962–2006 in the ENSEMBLES models. Therefore, this study offers important insights for AO predictions, even other climate variables predictions.

# Improving the Prediction of Arctic Oscillation by the Interannual Increment Approach

Dapeng Zhang[1,2], Yanyan Huang[1,2], Bo Sun[1,2]

1. Nanjing University of Information Science and Technology, Nanjing, China; 2. Nansen-Zhu International Research Center, Institute of Atmospheric Physics Chinese Academy of Sciences, Beijing, China

## a. Introduction

The main advantage of the interannual-increment approach is that the year-to-year increment (calculated by the value of current year minus the value of preceding year) amplifies the signals of interannual variability of predictors and/or predictant. To date, this approach has been utilized in many studies.

In this study, efforts have been made to improving the prediction of Arctic Oscillation (AO) by the interannual-increment approach.

## b. AO Prediction of ENSEMBLE
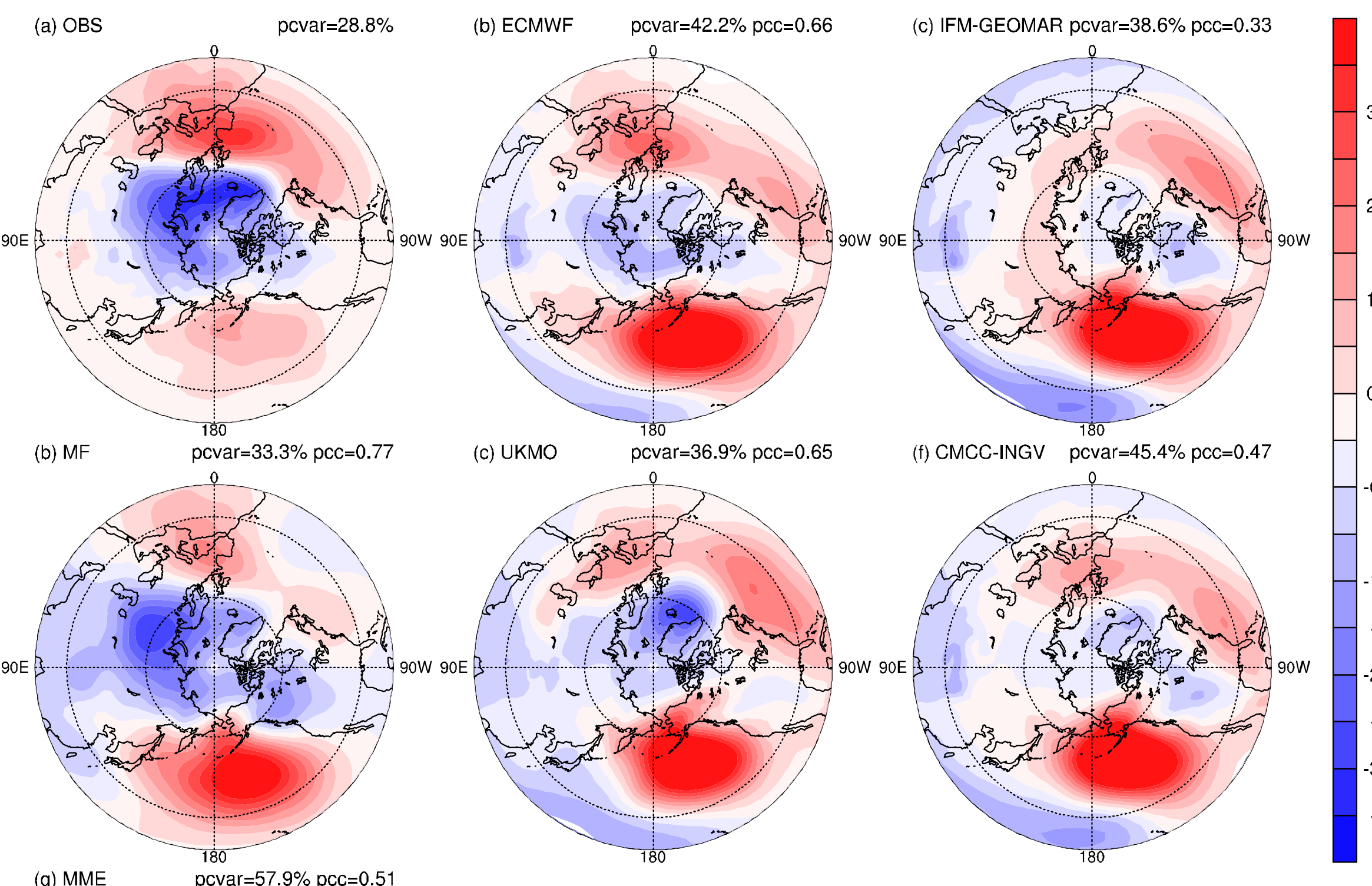


**Fig. 1**: The spatial patterns of the leading EOF mode of DJF sea level pressure anomalies (hPa) of north 20°N during 1961−2006 derived from observation (a) and ENSEMBLE (b-g). The pcvar and pcc represent the percent variance and spatial correlation coefficient of the leading EOF modes between observation and ENSEMBLE models, respectively.
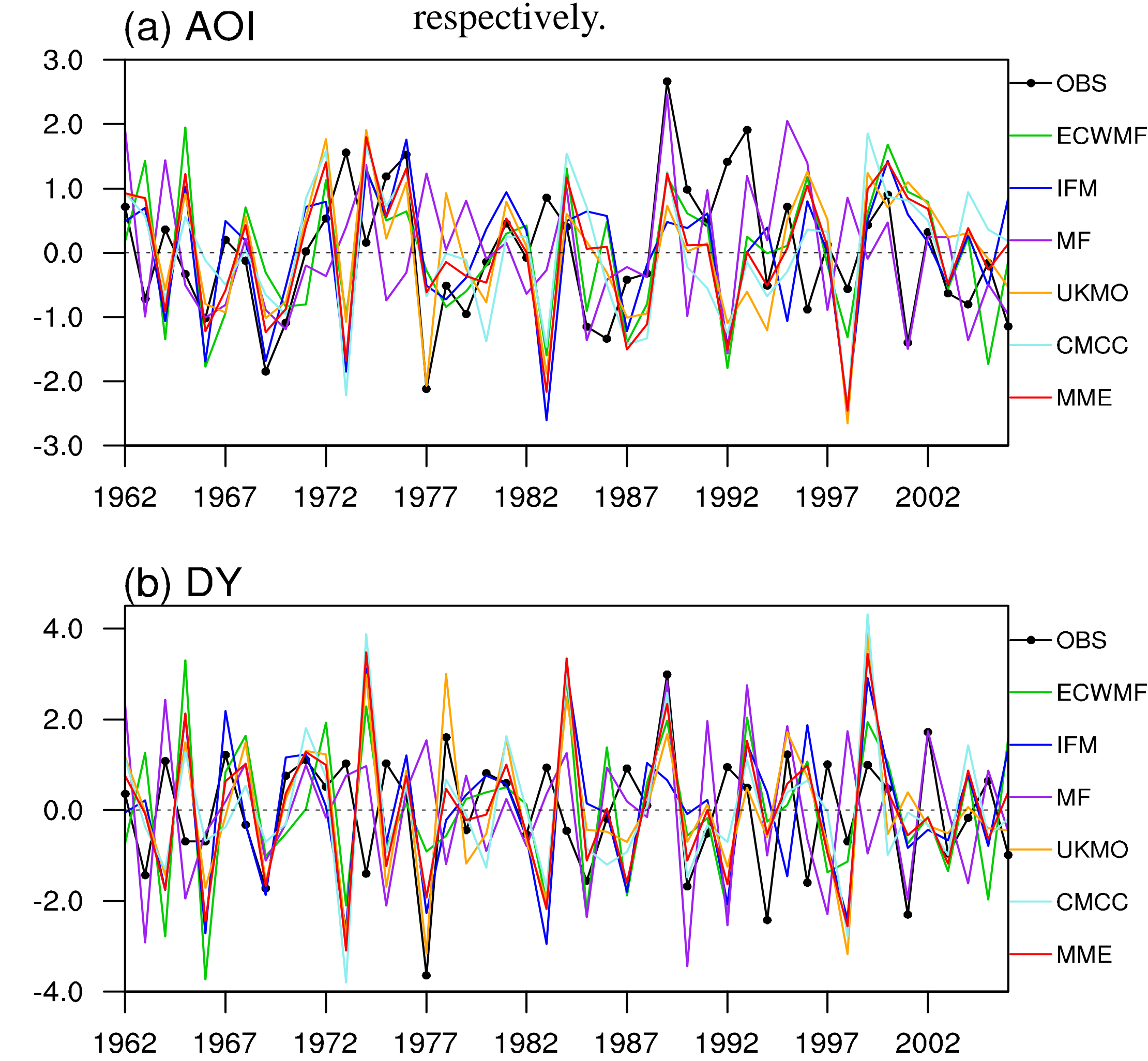


**Fig. 2**: The normalized DJF AOI (a) and DY of AOI (b) during 1962−2006 derived from observation and ENSEMBLE models, which are obtained by projecting the observed AO spatial pattern.

The ENSEMBLE model have bad performance in predicting the spatial pattern and interannual variation of AO, which demands improvements.

## e. Conclusion

**The good performance of this dynamical-statistical model indicates a capability of the interannual-increment approach for interannual prediction of the AO. Thus, the dynamical-statistical model combine interannual-increment approach gives a new clue for AO prediction and the short-term climate prediction.**

## c. Improvement

Preceding sea ice and concurrent SST are used as the predictors to improved the AO prediction for their significant impact on DJF AO. The dynamical-statistical model for DY_AOI prediction is established based on a multivariable regression method, as follows:

$$DY\_AOI_{predicted} = aDY\_SICI + bDY\_SSTI$$
$$AOI_{improved} = DY\_AOI_{predicted} + AOI_{obs-preceding}$$

**Predictor1 — Preceding Sea Ice**
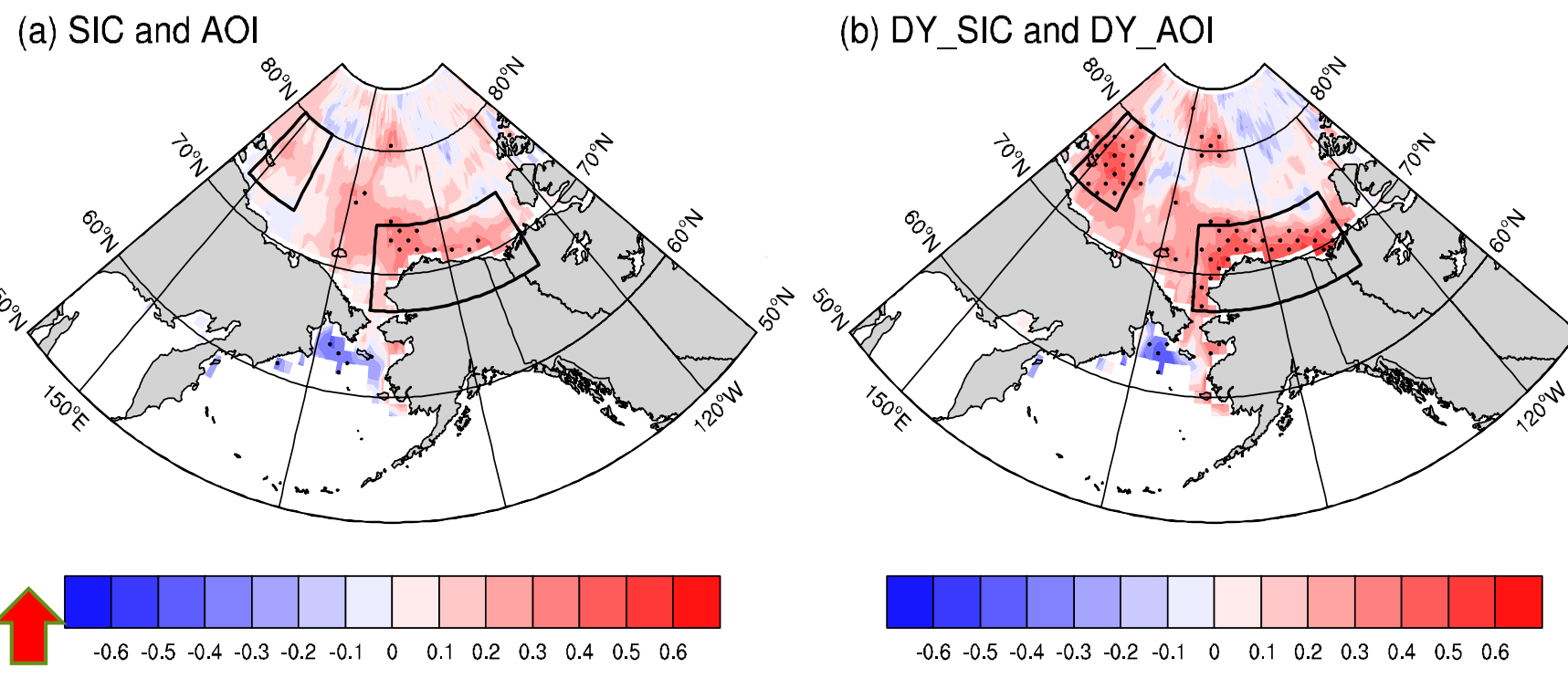


**Fig. 3**: (a) The correlation coefficients between the preceding SON sea ice concentration and DJF AOI derived from observation during 1961/62−2005/06. (b) As in (a), but for the DY of sea ice and the DY of AOI. The dotted areas indicate statistical significance at the 95% confidence level, based on a Student's t test.
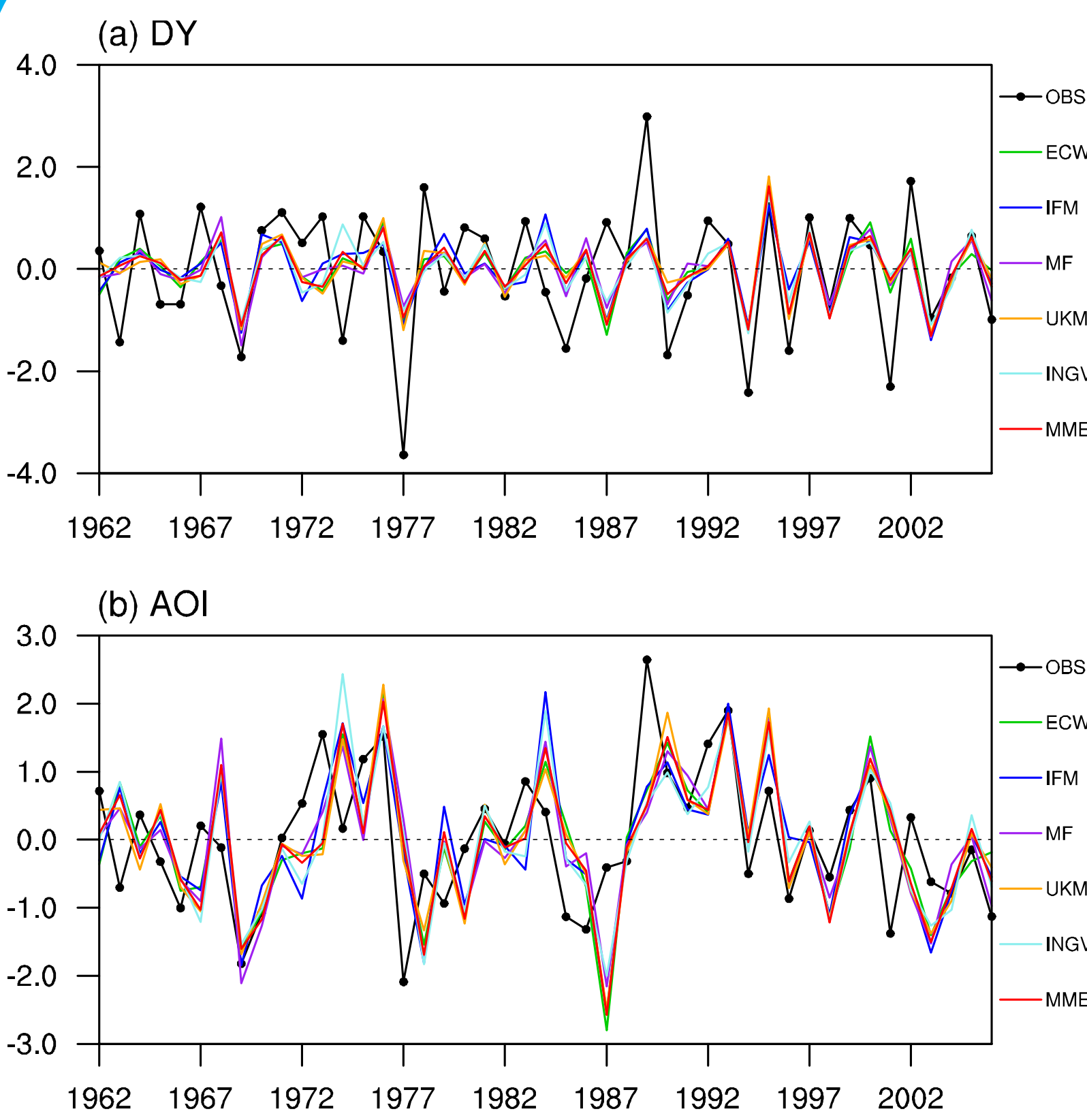
**Predictor2 — Concurrent SST**



**Fig. 4**: (left) The correlation coefficients between the observed DJF AOI and ENSEMBLE-predicted SST during 1962−2006. (right) As in (left), but for the DY of SST and the DY of AOI. The dotted areas indicate statistical significance at the 95% confidence level, based on a Student's t test.
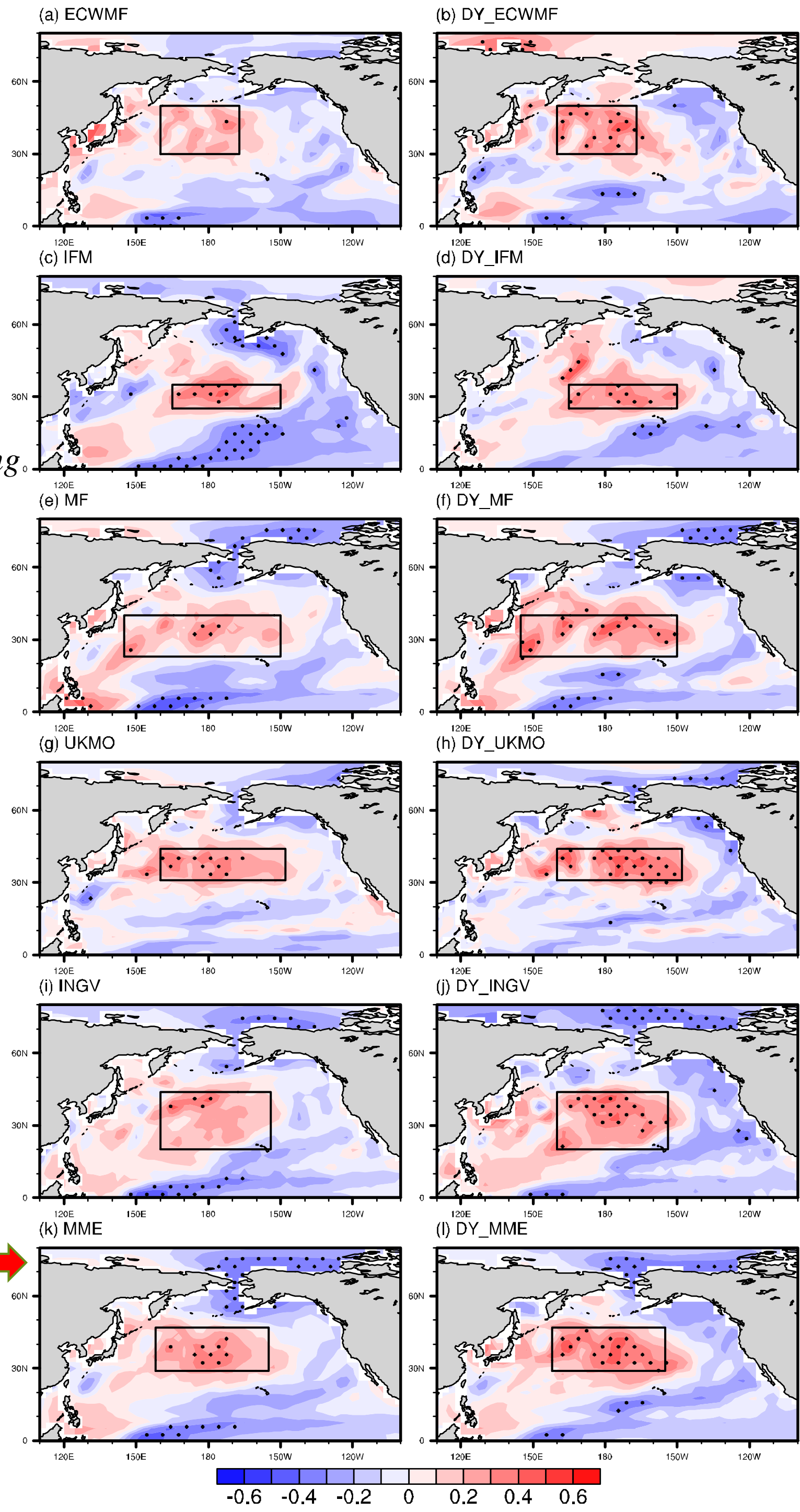
## d. Results

### Cross-validation



**Fig. 5**: Predicted and observed (a) DY of AOI and (b) AOI for 1962−2006, in which the predicted DY using the dynamic and statistical prediction model in the cross-validation.

Table 1 The correlation coefficients between the observed and predicted AOI, DY_AOI by the improved scheme (raw model) during 1962−2006 along with the improvement of RMSE in parentheses. Significance level at 95% (blue) and 99% (red) are based on a Student's t test with effective degrees of freedom.

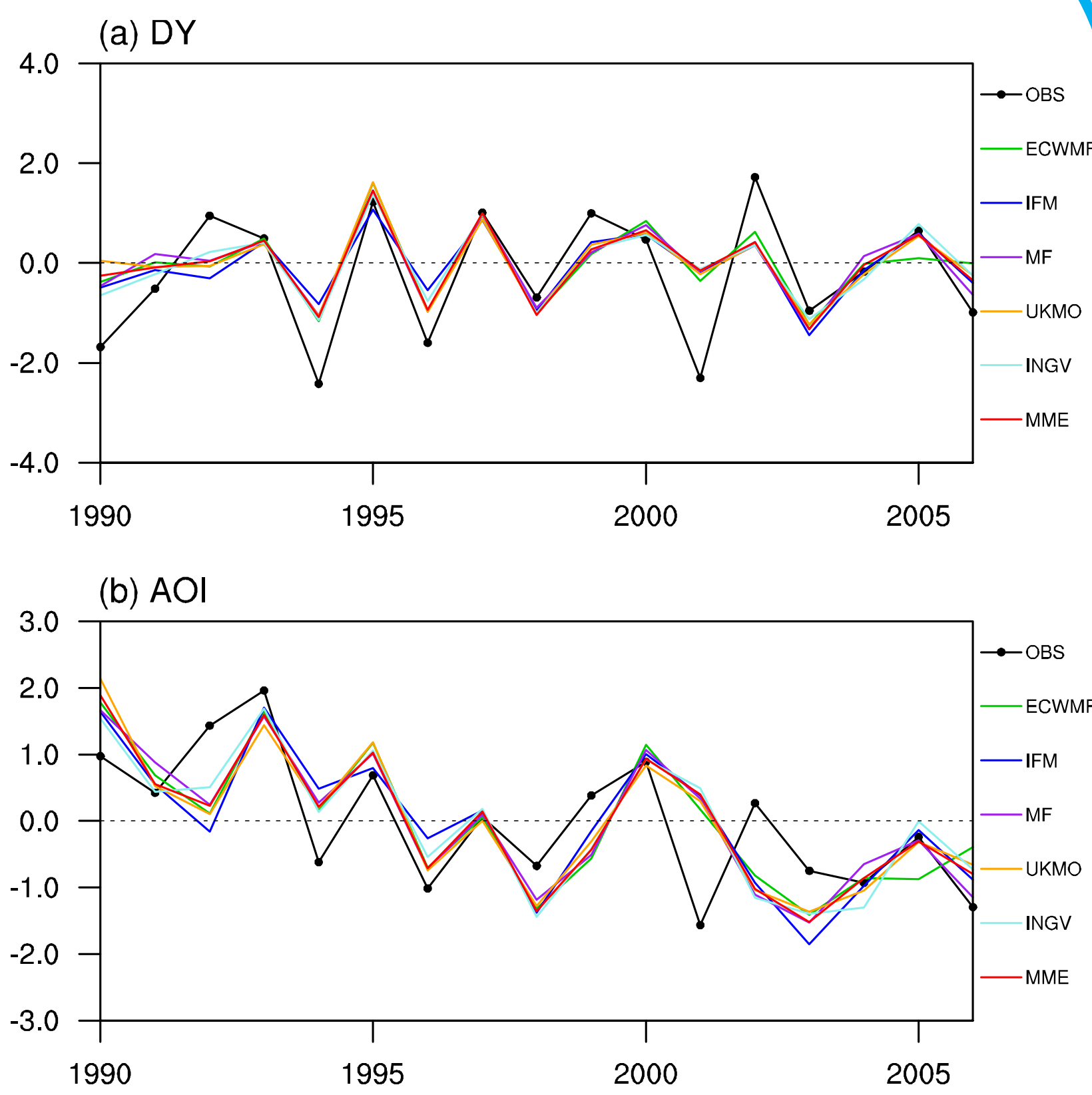| ENSEMBLE | Cross-Validation | | RMSE | |
|---|---|---|---|---|
| Model | AOI | DY_AOI | AOI | DY_AOI |
| ECWMF | 0.54(0.20) | 0.60(0.02) | 17% | 46% |
| IFM | 0.51(0.29) | 0.57(0.31) | 9% | 38% |
| MF | 0.54(0.33) | 0.59(0.30) | 8% | 40% |
| UKMO | 0.54(0.22) | 0.60(0.31) | 16% | 40% |
| INGV | 0.48(-0.05) | 0.52(-0.11) | 22% | 50% |
| MME | 0.51(0.36) | 0.55(0.33) | 3% | 37% |

### Hindcast



**Fig. 6**: Predicted and observed (a) DY of AOI and (b) AOI for 1990−2006, in which the predicted DY using the dynamic and statistical prediction model in the hindcast.

Table 2 The correlation coefficients between the observed and predicted AOI, DY_AOI by the improved scheme (raw model) during 1990−2006 along with the improvement of RMSE in parentheses. Significance level at 95% (blue) and 99%(red) is based on a Student's t test with effective degrees of freedom.

| ENSEMBLE | Hindcast | | RMSE | |
|---|---|---|---|---|
| Model | AOI | DY_AOI | AOI | DY_AOI |
| ECWMF | 0.66(0.09) | 0.76(0.26) | 41% | 58% |
| IFM | 0.62(0.08) | 0.73(0.35) | 26% | 37% |
| MF | 0.67(0.31) | 0.76(0.40) | 31% | 53% |
| UKMO | 0.65(-0.07) | 0.72(0.34) | 35% | 39% |
| INGV | 0.67(0.10) | 0.79(-0.08) | 30% | 54% |
| MME | 0.66(0.15) | 0.75(0.39) | 29% | 42% |

The dynamical-statistical model demonstrates a considerable capability for improving the AOI prediction of ENSEMBLE, with most the improved correlation coefficients significant at 99% confidence level and the large reduce of RMSE in cross-validation and hindcast.

**Reference**: Zhang, D., Huang, Y., & Sun, B. (2019). Verification and improvement of the capability of ENSEMBLES to predict the winter Arctic Oscillation. *Earth and Space Science*, 6 https://doi.org/10.1029/2019EA000771

**Correspondence to:**
Y. Huang,
huangyy@nuist.edu.cn

# Verification and Improvement of the Capability of ENSEMBLES to Predict the Winter Arctic Oscillation

**Dapeng Zhang[1,2]** [iD], **Yanyan Huang[1,2]** [iD], and **Bo Sun[1,2]** [iD]

[1]Collaborative Innovation Center on Forecast and Evaluation of Meteorological Disasters/Key Laboratory of Meteorological Disaster, Ministry of Education, Nanjing University of Information Science and Technology, Nanjing, China, [2]Nansen–Zhu International Research Centre, Institute of Atmospheric Physics, Chinese Academy of Sciences, Beijing, China

**Abstract** The winter Arctic Oscillation (AO) is important for understanding the Northern Hemisphere climate variability and predictability. However, ENSEMBLES models produce inconsistent predictions when applied to the interannual variability of the 1962–2006 winter AO. In this study, the interannual increment of the winter AO index (DY_AOI) during 1962–2006 is first improved by a dynamical-statistical model with two predictors: the preceding autumn Arctic sea ice and the concurrent winter ENSEMBLES-predicted sea surface temperature over the North Pacific. Next, the improved final AOI is obtained by adding the improved DY_AOI to the preceding observed AOI. Because the interannual increment approach can amplify prediction signals and takes advantage from the previous observed AOI, this method shows promise for significantly improving the interannual variability prediction capabilities of the winter AO during 1962–2006 in the ENSEMBLES models. Therefore, this study offers important insights for AO predictions, even other climate variables predictions.

## 1. Introduction

Thompson and Wallace (1998) found that the Arctic Oscillation (AO), which is also known as the Northern Annular Mode, is the primary mode of the extratropical atmospheric circulation in the Northern Hemisphere (NH). The AO is characterized by an out-of-phase relationship between the midlatitudinal and high-latitudinal parts of the atmosphere in the NH. The positive phase of the AO is associated with positive (negative) anomalies of SLP in the midlatitudes (high latitudes) and vice versa; the AO has a zonally symmetric pattern (Thompson & Wallace, 2000). This pattern of the AO represents a barotropic structure that can be observed from the ground up to the lower stratosphere (Thompson & Wallace, 1998, 2001).

The AO has a larger amplitude and meridional scale in the cold season (Thompson & Wallace, 2000) throughout the year. Consequently, the winter AO produces a stronger exchange of mass and energy between the midlatitudes and the Arctic atmosphere than the other season AO and has a noticeable effect on the temperature and precipitation of the Northern Hemisphere (He et al., 2017, 2019; Wettstein & Mearns, 2002). Early studies suggested that the winter AO has an important influence on the climate of East Asia by impacting the Siberian High, westerly winds, and blocking frequencies (Gong & Wang, 2003; He et al., 2017; Li et al., 2014). Specifically, a positive phase of the winter AO is associated with a weakened East Asian winter wind, leading to weaker cold wave activities and warmer conditions in East Asia as well as increased (decreased) winter precipitation in the southern (northern) regions of China (He & Wang, 2013; Li et al., 2018; Zhu et al., 2018). The winter-spring AO also influences spring dust storms, temperature, and precipitation (Gong et al., 2006; He et al., 2017; Mao et al., 2011) and even summer rainfall in China (Gong & Ho, 2003). Moreover, the winter AO can also lead to extreme weather events (He & Wang, 2016). The winter AO in 2008 played an important role in a major winter storm event in South China that affected 100 million people and led to 100 billion yuan in economic losses (Zhao et al., 2008). Considering the significant influence of the winter AO on NH climate predictability and the predictability of extreme weather events, it is important to obtain reliable predictions of the winter AO.

The main method for predicting the AO is the numerical model. Previous studies found that the National Centers for Environmental Prediction Climate Forecast System version 2 can predict the winter AO up to two months in advance (Riddle et al., 2013). However, this predictive capability is based on the ensemble

average of 188 hindcasts of the Climate Forecast System version 2, which requires huge computing resources. In addition, Kang et al. (2014) assessed six state-of-the-art seasonal forecast models that accurately predicted the winter AO for 1997–2010; however, they were less accurate in predicting the winter AO for 1983–1996. The predictability of the AO by DEMETER project was also evaluated; the seven models in this project succeeded in predicting the AO pattern but failed to predict the temporal variability of the AO (Qian et al., 2011).

It is revealed that the larger the variability is, the better predictability will be (Sun & Wang, 2013). Recently, considering the quasi-biennial oscillation of climate variables, the interannual increment approach was proposed to improve seasonal to interannual climate predictions (Fan et al., 2008). Instead of focusing on the anomalies of a variable relative to climatology, a strategy that is used in the conventional prediction approach, the interannual increment approach uses the year-to-year increment (calculated by the value of the current year minus the value of preceding year, called the DY) of variables as the predictant. Then, the final predicted variable result is obtained by adding the predicted DY of the variable to the observed value from the previous year. Specifically, if a climate variability (Y) has a characteristic of quasi-biennial oscillation, $Y_i$ and $Y_{i-1}$ represent the variable in the current and previous year, respectively, then $Y_i = C + P_i$ and $Y_{i-1} = -C + P_{i-1}$ where $P_i$ and $P_{i-1}$ represent a disturbance in C. After ignoring the disturbance, the year-to-year increment is $DY_i = Y_i - Y_{i-1} \approx 2C$, suggesting that the amplitude of a variable in the form of the year-to-year increment is twice the value of the anomaly (Fan et al., 2008), which is conductive to short-term climate prediction (Sun & Wang, 2013). Meanwhile, because the final predicted variable is obtained by including the observed value from previous year, which contains the interdecadal signals, the interannual increment approach is able to capture the interdecadal variability of the variable (Fan et al., 2012; Huang et al., 2014). To date, the interannual increment approach has successfully predicted winter/summer temperature and rainfall over China (Fan et al., 2008; Fan & Wang, 2010), and East Asian winter/summer winds and winter haze days (Fan et al., 2012; Tian et al., 2018; Yin & Wang, 2016). This interannual increment approach is also used to improve the large-scale atmospheric circulation predictions of numerical models that focus on climate patterns such as the Asian-Pacific Oscillation (Huang et al., 2014), the North Atlantic Oscillation (Fan et al., 2016; Tian & Fan, 2015), and the Antarctic Oscillation (Zhang et al., 2019). Moreover, recent studies have suggested that the interannual increment approach has particularly effective predictive capabilities with respect to extreme weather events (Qian et al., 2018). However, the utility of this interannual increment approach for predicting the AO has not yet been examined.

ENSEMBLES is a European Union-funded integrated project that intends to develop an ensemble prediction system for climate change based on the principal state-of-the-art, high-resolution global models developed in Europe (Doblas-Reyes et al., 2009). The five leading European global coupled climate models of the ENSEMBLES project are well suited to evaluate climate predictability (Li et al., 2012). Previous studies have suggested that ENSEMBLES has a strong ability to predict the East Asian winter monsoon and the western North Pacific summer climate, including precipitation and sea surface temperatures (SSTs; Li et al., 2012; Weisheimer et al., 2009; Yang & Lu, 2014). Meanwhile, the 46-year hindcasts of 1961–2006 in ENSEMBLES offer an opportunity to understand the predictability of climate variables and their stationarity. However, how do the ENSEMBLES models predict the AO? Can the interannual increment approach improve AO predictions? All of these issues are worth explored.

In this study, the ability of ENSEMBLES to predict the winter AO is assessed, and a dynamical-statistical model is established to improve the ability of ENSEMBLES to predict the winter AO based on the interannual increment approach. The data and methods are introduced in section 2. Section 3 evaluates the ability to predict the AO using ENSEMBLES. In section 4, the dynamical-statistical model is established to improve AO predictions of ENSEMBLES and is validated by the methods of cross-validation and independent hindcasting. Conclusions and discussions are presented in section 5.

## 2. Data and Methods

### 2.1. Data

The ENSEMBLES project includes five coupled atmosphere-ocean-land models developed by the European Centre for Medium-Range Weather Forecasts, the Leibniz Institute of Marine Sciences at Kiel University (IFM), Météo-France (MF), the UK Met Office (UKMO), and the Euro-Mediterranean Center for Climate

Change (CMCC). We use the monthly hindcasts of the SLP and SST for December-January-February (DJF) during 1961−2006 in the five ENSEMBLES models. For each year, the monthly hindcasts are initialized on 1 November with nine members for each model. The multimodel ensemble (MME) is calculated by taking a simple equal weight average of the five models.

The observed data used in this study include monthly SLP data (2.5° × 2.5°) derived from the National Centers for Environmental Prediction Reanalysis I product (Kalnay et al., 1996), SSTs from the NOAA Extended Reconstructed SST version 3b (2° × 2°) data set (Smith et al., 2008), and sea ice concentration (SIC) data (1° × 1°) from the Met Office Hadley Centre (Rayner et al., 2003). All data sets are interpolated to 2.5° × 2.5° horizontal resolution using bilinear interpolation. Considering that this study focuses on inter-annual variability, all of the data sets from 1961 to 2006 are detrended.

The Arctic Oscillation Index (AOI) of winter (DJF) is defined as the time series of the leading empirical orthogonal function (EOF) mode of winter SLP anomalies north of 20°N (Thompson & Wallace, 1998). For obtaining the best model performance, the ENSEMBLES-predicted AOI in this study is obtained by projecting the observed AO spatial pattern (the leading EOF mode) onto the ENSEMBLES-predicted SLP.

### 2.2. Methods

In this study, a dynamical-statistical model is established to improve the ENSEMBLES-predicted AOI. Assuming that two predictors of sea ice (SIC) and SST are selected and the relationships of the winter AO with SST and SIC are analyzed. Afterward, based on the multivariable regression method, the dynamical-statistical model for the DJF DY of AOI (DY_AOI) prediction is established as follows:

$$DY\_AOI = aDY\_SICI + bDY\_SSTI \tag{1}$$

where DY_SICI represents the observed preceding SON SIC for the DY form; DY_SSTI is the ENSEMBLES-predicted concurrent SST for the DY form; and $a$ and $b$ are the corresponding regression coefficients for SON sea ice and the DJF SST, respectively. In this way, dynamical-statistical models are established for each of the ENSEMBLES models.

Both the cross-validation method and the independent hindcast method are used to validate this dynamical-statistical model. The cross-validation method predicts the predictand for two specific years via a model built from the sample omitting these two years; this approach is known as the two-year-out cross-validation (Michaelsen, 1987). Specifically, we use the data during 1964−2006 to establish the dynamical-statistical model to predicted the DYs of AOI (DY_AOIs) in 1962 and 1963. Then the improved AOIs from 1962 and 1963 are obtained by adding the predicted DY_AOIs to the observed AOI from 1961 and 1962, respectively. And so on, we can get the improved AOI from 1962 to 2006. Independent hindcasts for 1990−2006 also predict the DY_AOIs in the target year among the 17 years, while a model is established on a 29-year sliding window prior to the target year. Then the final improved AOIs are also got by adding the predicted DY_AOIs to the observed AOIs from previous year.

The correlation coefficient and the root-mean-square error (RMSE) are also used in this study. The statistical significance of correlation coefficients is estimated using Student's $t$ test. The number and independence of samples often have nontrivial influence on their significance. The effective number of independent samples (degrees of freedom) is calculated by Monte Carlo simulation and testing, which is measured by the quotient of the number dividing the autocorrelations at different lags of the time series, removing the autocorrelation of the independent samples or time series (Livezey & Chen, 1983). In this study, the improved DY_AOI and AOI in cross-validation and independent hindcast are tested with effective degrees of freedom (Tables 2 and 3).

## 3. The Predictive Capability of ENSEMBLES

Considering that the definition of the AO mode in this study is the leading EOF mode of the SLP, the SLP predictions in ENSEMBLES are evaluated first. Figure 1 shows the climatological DJF mean SLP north of 20°N during 1961−2006 derived from observations and the ENSEMBLES models. The SLPs predicted by ENSEMBLES are consistent with observations of the spatial pattern of the DJF mean SLP in the NH. Specifically, the position and intensity of the Mongolian high, the Aleutian low, and the Icelandic low are
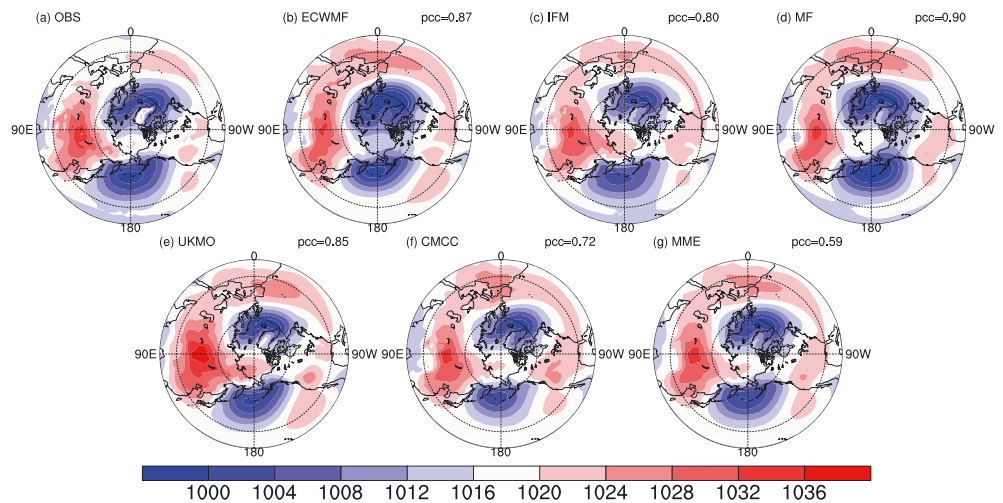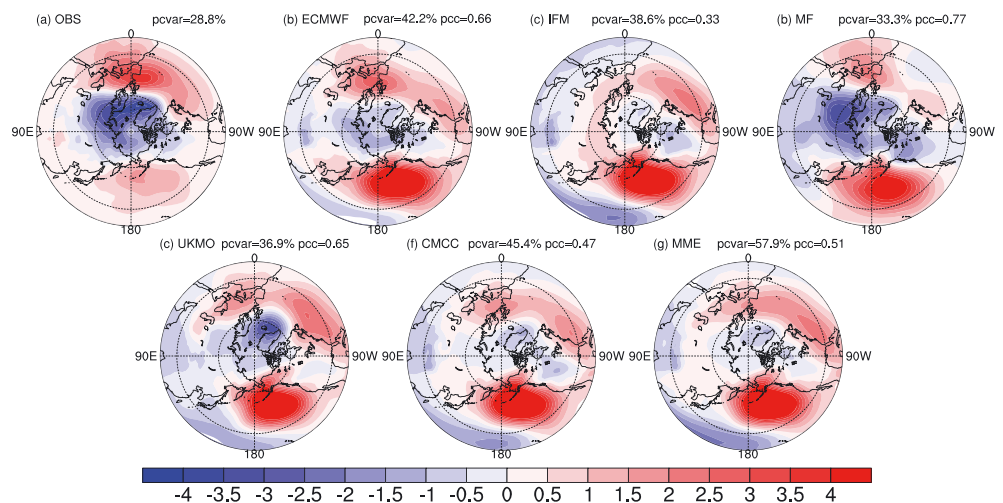
**Figure 1.** The DJF mean sea level pressure (units: hPa) north of 20°N during 1961–2006 derived from the (a) observations, (b) ECWMF, (c) IFM, (d) MF, (e) UKMO, (f) CMCC, and (g) MME.

well predicted by ENSEMBLES models relative to the observed results. All of the spatial correlation coefficients (uncentered) between the ENSEMBLES predictions and the observations for the DJF mean SLP are above the value of 0.90 significance at the 95% confidence level except for the correlation coefficients from the ECWMF model (0.88), which overestimates the intensity of the Icelandic low. Moreover, all of the models show a 4−8-hPa overestimation of the mean SLP over the European and Atlantic regions, where the observed SLPs are mostly below 1,020 hPa (Figure 1a), while the ENSEMBLES-predicted SLPs are mostly above 1,020 hPa (Figures 1b–1g).

The EOF analysis is applied to each ENSEMBLES model to evaluate the AO modes predicted by these models. The leading EOF modes are shown in Figure 2, which is characterized by opposite anomalies in the Arctic Ocean and the midlatitudinal oceans (the North Atlantic Ocean and the North Pacific Ocean), representing the zonally symmetric pattern of the AO. Although all ENSEMBLES models are able to produce this opposite pattern well, they tend to overestimate the anomalies in the North Pacific and underestimate the anomalies in the North Atlantic and Arctic. Correspondingly, the spatial correlation coefficients between the observations and the forecasts reflect the inconsistent predictive capabilities of these models. The MF, ECWMF, and UKMO models have comparable spatial correlation coefficients (uncentered) that are higher than 0.60, indicating that these models perform reasonably in identifying the positions of anomalies in the Arctic Ocean, North Atlantic Ocean, and North Pacific Ocean in comparison to the observations. In contrast, the IFM and CMCC models and MME do not capture the positions and intensities of the anomalies in the Arctic and North Atlantic. Generally, the ENSEMBLES models can capture the zonally symmetric pattern of the AO mode, but place much emphasis on the center in North Pacific. Furthermore, the MF, UKMO, and ECWMF models exhibit more reasonably predictive capabilities for AO prediction than the other models.

Figure 3 displays the DJF AOIs and the DY_AOIs from 1962 to 2006 that were obtained from observations and the ENSEMBLES forecasts. From above analysis, the ENSEMBLES project shows relatively high biases in its predictions of AO spatial pattern; the ENSEMBLES-predicted AOIs are obtained by projecting the observed AO spatial pattern (Figure 2a) onto the ENSEMBLES-predicted SLP to get optimal models forecasts. The MME shows relatively consistence with the observed AOI with a correlation coefficient of 0.36, significant at 99% confidence level (Table 1), notwithstanding the opposing relationship in the 1960s and 1990s. However, the correlation coefficients between the observed and predicted AOIs are 0.20, 0.29, 0.33, 0.22, and −0.05 for the ECWMF, IFM, MF, UKMO, and CMCC models, respectively (Table 1). Only the IFM and MF-predicted the correlation coefficients are statistically significant at 95% confidence level, reflecting the uneven performance of the above models in predicting the interannual variation of the DJF AO (Figure 3a). The corresponding DY_AOIs also reflect the uneven capabilities of most of the forecasts, which exhibit inconsistent relationships between the observed and predicted results; correlation coefficients are

**Figure 2.** Spatial patterns of the leading EOF mode of DJF SLP anomalies (units: hPa) north of 20°N during 1961–2006 derived from the (a) observations, (b) ECWMF, (c) IFM, (d) MF, (e) UKMO, (f) CMCC, and (g) MME. The abbreviations pcvar and pcc represent the percentage variance and spatial correlation coefficient of the leading EOF modes between the observations and the models, respectively.

0.02 and 0.11 for the ECWMF and CMCC models, respectively (Table 1). Meanwhile, the IFM, MF, UKMO, and MME models have correlation coefficients of 0.31, 0.30, 0.31, and 0.33, significant at the 95% confidence level, respectively, indicating their relative ability to predict the DY of the AOI. Therefore, the ECWMF and CMCC models have poor performance in predicting the interannual variation of AOI. Although the IMF, MF, and MME models show some predictive capabilities for the AOI and the DY of the AOI, the ENSEMBLES predictions for the DJF AO are far from reliable and require improvements.
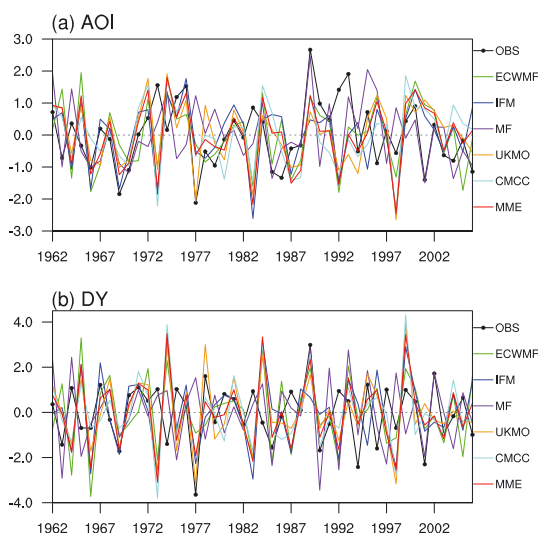
## 4. Improvements to AO Prediction

The AO has a two-year period for the wavelet analysis of the winter AOI from 1961 to 2006 in Figure 4, indicating that it is reasonable to use the interannual increment approach to improve the AO prediction. Additionally, considering the poor performance of most ENSEMBLES models in DJF AO predictions, the combination of a dynamical-statistical model and an interannual increment approach is used to improve the AO predictions. According to this method, a dynamical-statistical model is established to improve the DY of the AOI for each model of ENSEMBLES. Then, the final predicted AOI is generated by adding the improved DY of the AOI to the observed AOI of the previous year. The predictors used in this model, the approach of this dynamical-statistical model, and the validation and hindcast of this model are discussed as follows.

### 4.1. The Predictors and Associated Mechanisms



**Figure 3.** The normalized (a) DJF AOI and (b) DY_AOI during 1962–2006 derived from the observations, ECWMF, IFM, MF, UKMO, CMCC, and MME.

Two types of predictors can be used to establish the dynamical-statistical model. One is the observed preceding predictor, which has a lead-lag relationship with the predictand, that is, the DJF AO. The other is the concurrent predictor that is well predicted by numerical models. It is suggested that sea ice (Liu et al., 2012), SST (Marshall et al., 2001), and snow cover (Saito & Cohen, 2003) contribute to the interannual variability of winter AO. The changes in these boundary conditions have influence on the upward propagation of planetary waves from the lower troposphere to the stratosphere, strengthening or weakening the stratospheric polar vortex. Then, there is a process of downward propagation of stratospheric AO anomalies to troposphere, which is modulated by the waveguide for

**Table 1**
*Correlation Coefficients Between the Observed and Directly Predicted AOIs and the Corresponding DY Form (DY_AOI) in the ENSEMBLES Project for 1962–2006 (1990–2006) Along With the RMSEs*

| ENSEMBLES model | Correlation coefficients | | RMSE | |
|---|---|---|---|---|
| | AOI | DY_AOI | AOI | DY_AOI |
| ECWMF | 0.20 (0.09) | 0.02 (0.26) | 1.26 (1.42) | 1.91 (2.04) |
| IFM | 0.29* (0.08) | 0.31* (0.35) | 1.19 (1.21) | 1.68 (1.44) |
| MF | 0.33* (0.31) | 0.30* (0.40) | 1.15 (1.21) | 1.74 (1.81) |
| UKMO | 0.22 (−0.07) | 0.31* (0.34) | 1.24 (1.38) | 1.71 (1.48) |
| CMCC | −0.05 (0.10) | −0.11 (−0.08) | 1.45 (1.15) | 2.19 (1.84) |
| MME | 0.36** (0.15) | 0.33* (0.39) | 1.13 (1.19) | 1.70 (1.51) |

*Note.* "*" and "**" indicate statistical significance at the 95% and 99% confidence level, based on Student's *t* test.

planetary-scale waves, contributing to a certain AO phase/amplitude (Baldwin & Dunkerton, 1999; Xu, He, et al., 2018). Accordingly, the preceding September-October-November (SON) Arctic sea ice data and concurrent DJF SST data are selected for the dynamical-statistical model; these data are derived from the observational data and the ENSEMBLE predictions, respectively.

The variability of highly reflective sea ice could affect the radiation balance, the freshwater budget, and deep-water formations along with the surface flux of heat and moisture between the ocean and the atmosphere that modulates atmospheric circulation (Lin & Li, 2018; Stammerjohn & Smith, 1997; Xu, Li, et al., 2018). It is suggested that a reduction in SON Arctic sea ice could lead to the development of the negative phase of the DJF AO (Kim et al., 2014; Liu et al., 2012). The mechanism can be explained that the decreased sea ice cover in Arctic strengthens the upward planetary wave propagation with wave number of 1 and 2. Then, the upward waves weaken the stratospheric polar vortex, inducing a negative phase of AO at the troposphere/surface though (Kim et al., 2014) with a downward process above mentioned (Baldwin & Dunkerton, 1999). The positive correlation relationship between SON Arctic sea ice and DJF AO is also shown in Figures 5a and 5b. Therefore, the preceding SON Arctic sea ice can be considered a predictor for the dynamical-statistical model.

Figure 5 shows the distribution of correlation coefficients between the preceding SON SIC and the DJF AOIs. A positive relationship between the Arctic SON SIC and the winter AOI is displayed in Figure 5a. The significant influence of the autumn sea ice on the winter AO is particularly evident in the Beaufort Sea (Figure 5a). In addition, the correlation coefficients between the corresponding DY_SICs and DY_AOIs are shown in Figure 5b. The DY_SICs and DY_AOIs indicate a more significant correlation in the East Siberian Sea and the Beaufort Sea than is demonstrated by the above-mentioned correlation between the SIC and the AOIs.

The increased correlation shown in Figure 5b demonstrates the advantage of the interannual increment approach for amplifying the signals of interannual variability. Thus, the area-weighted areal mean SON DY_SIC in two key regions is defined as the sea ice index (DY_SICI), shown in Region-1, covering (73°N−80°N, 147°E−164°E), and Region-2, covering (67°N−74°N, 130°W−170°W), for the positive correlation coefficients between the DY_SIC and the DY_AOI are associated with the East Siberian Sea and the Beaufort Sea, as shown in Figure 5b. Hereafter, the DY_SICI for SON sea ice is defined as the sum of the area-weighted areal mean SON DY_SICs in Region-1 and Region-2, which has a significant correlation coefficient of 0.55 with the observed DY_AOI. Thus, the DY_SICI will be used in the dynamical-statistical model for DY_AOI predictions.

Many previous studies suggest that the SST has a significant influence on atmospheric circulation (Han et al., 2017; Li et al., 2017; Marshall et al., 2001). In particular, the association between the extratropical Pacific SST and atmosphere is described (Li et al., 2015). Li et al. (2015) revealed that positive anomalies in the midlatitudinal North Pacific tend to
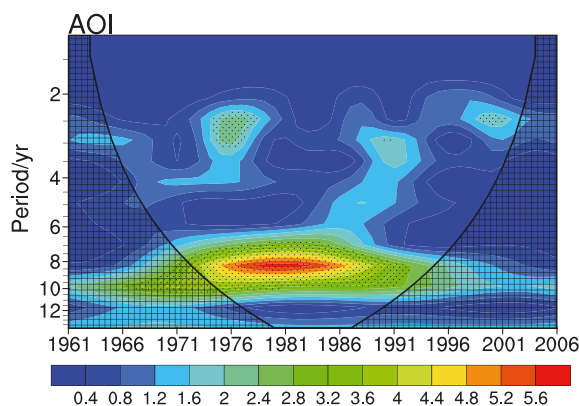
**Figure 4.** Wavelet analysis of the DJF AOI for the period 1961–2006. Dotted regions indicate significant variability at the 90% confidence level estimated by a red noise process, and the parabola indicates the "cone of influence."
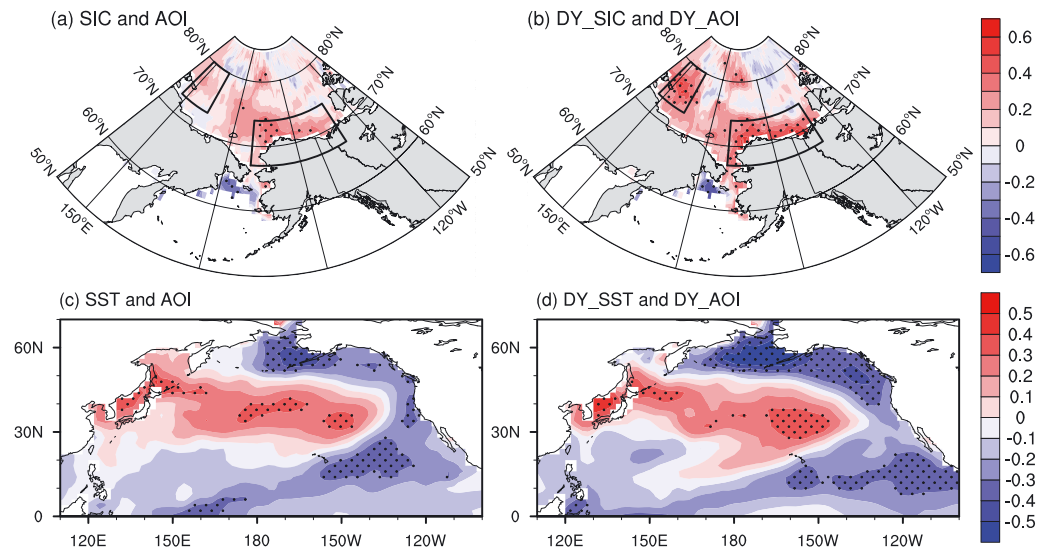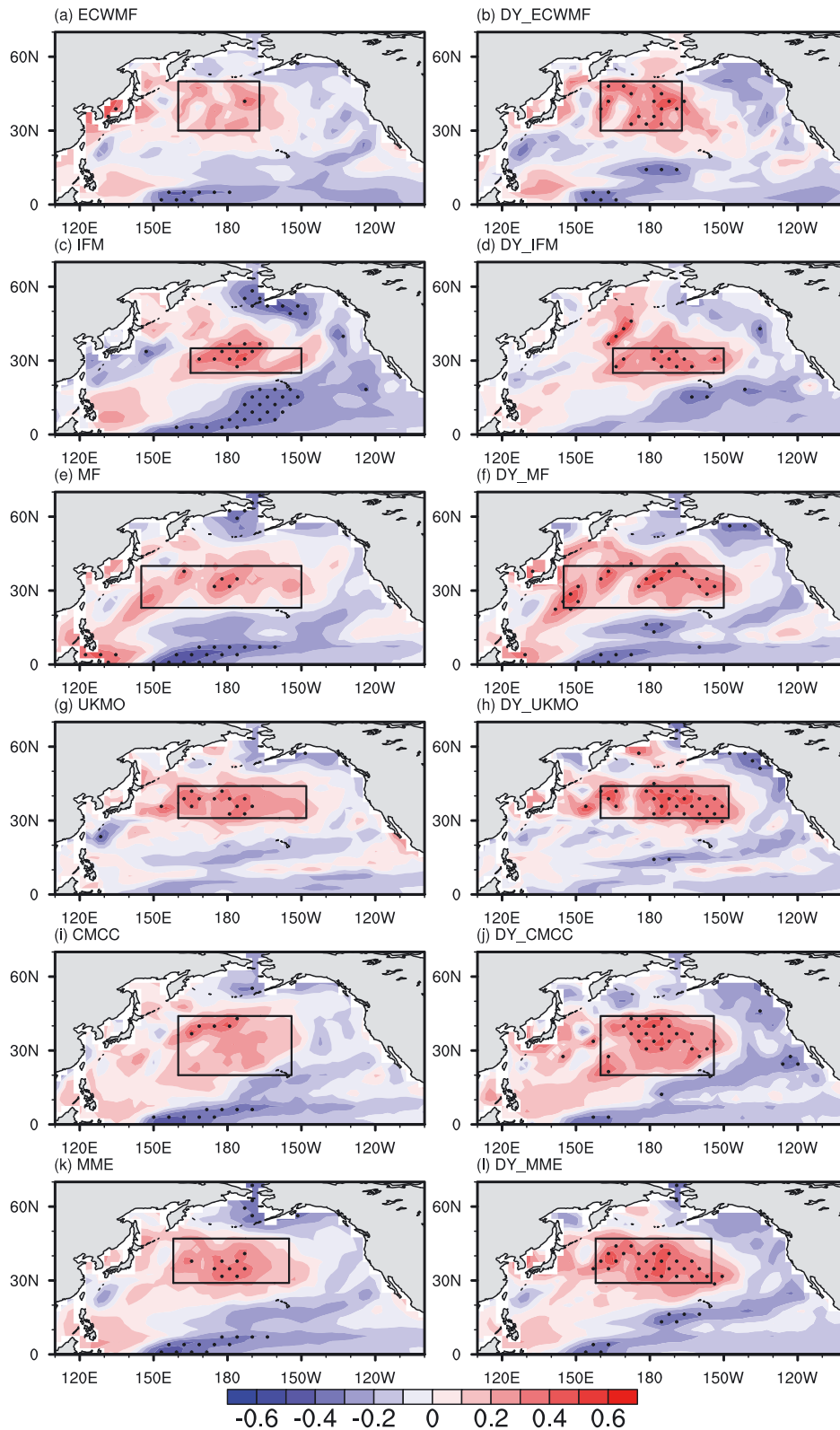
**Figure 5.** (a) Correlation coefficients between the preceding SON SIC and the DJF AOI derived from observations during 1962/1963–2005/2006. (b) Same as in (a) but for the DY of sea ice and the DY of the AOI. Dotted areas indicate statistical significance at the 95% confidence level, based on Student's *t* test. The black curvilinear rectangles represent the key regions where the SON SIC influences the DJF AO. (c and d) Same as in (a) and (b) but for observed DJF SST and AOI.

enhance the equatorward planetary wave propagation, inducing a strengthened poleward meridional eddy momentum flux. Meanwhile, negative SST anomalies in the high-latitudinal North Pacific tend to weaken the upward planetary wave propagation, implying a weak poleward eddy heat flux. Consequently, the upper level polar night jet is strengthened and polar vortex become colder, suggesting an intensified polar vortex, following a positive phase of AO at the troposphere/surface (Mitchell et al., 2013). The mechanism indicates a significant positive (negative) correlation relationship between the concurrent midlatitudinal (high-latitudinal) Pacific SST and DJF AO, which can be observed in Figures 5c and 5d. Considering the significant influence of the concurrent SST on the DJF AO, the ENSEMBLES-predicted SST may be used as another concurrent predictor in the dynamical-statistical model.

The distribution of correlation coefficients between the North Pacific SSTs (DY_SST) and the AOIs (DY_AOI) derived from the ENSEMBLES models and winter observations are displayed in Figure 6. Compared to the observations (Figures 5c and 5d), all the ENSEMBLES models predict the significant positive correlation between observed AOI and predicted SSTs in the midlatitudinal Pacific of the NH and fall to predict the significant negative correlation in the Bering Sea (Figure 6). Moreover, large areas with significant positive correlation coefficients between the observed AOIs and the predicted SSTs are found in the midlatitudinal North Pacific for the IFM (Figure 6c) and UKMO (Figure 6g) models, and MME (Figure 6k). However, for the ECWMF (Figure 6a), MF (Figure 6e), and CMCC (Figure 6i) models, the SSTs have an insignificant relationship with the observed AOIs. Meanwhile, the observed DY_AOI and predicted DY_SST exhibit more significant correlations than the previously described predictions in the midlatitudinal North Pacific for all the ENSEMBLES models (the right column of Figure 6). Compared to the correlation coefficients between the AOIs and the SSTs (the left column of Figure 6), the correlation coefficients for the DY form are more significant and extensive in the midlatitudes of the Pacific, which reflects the significant relationship between the DJF AOI and the concurrent SST revealed by the interannual increment approach.

The area-weighted areal mean DJF DY_SSTs of the ENSEMBLES predictions in key regions are computed as SST indices (DY_SSTI); Region-3 covers the midlatitudes of the North Pacific for the ECWMF (30°N−50°N, 160°E−173°W), IFM (25°N−35°N, 165°E−150°W), MF (23°N−40°N, 145°E−150°W), UKMO (31°N−44°N, 160°E−148°W), and CMCC (20°N−44°N, 160°E−146°W) models and the MME (27°N−43°N, 153°E−145°W), as shown in the right column of Figure 5. The same key regions (25°N−45°N, 160°E−150°W) over midlatitudinal North Pacific in all ENSEMBLES models have also been used to

**Figure 6.** Correlation coefficients between the observed DJF AOIs and the model-predicted SSTs during 1962–2006 for the (a) ECWMF, (c) IFM, (e) MF, (g) UKMO, (i) CMCC, and (k) MME. (b, d, f, h, j, and l) Same as in (a), (c), (e), (g), (i), and (k), respectively, but for the DY of the SST and the DY of the AOI. Dotted areas indicate statistical significance at the 95% confidence level, based on Student's *t* test. The black curvilinear rectangles represent the key regions where the SST influences the DJF AO.
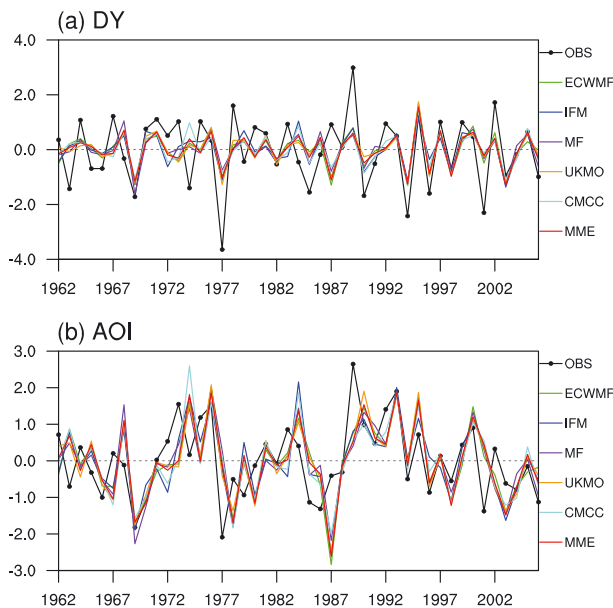
**Figure 7.** Predicted (a) DY of the AOI and (b) AOI during 1962–2006 for the observations, ECWMF, IFM, MF, UKMO, CMCC, and MME, in which the predicted DY uses the dynamical–statistical prediction model in the cross-validations.

improve the DY_AOI, showing little difference with the improved results of different regions for different models. Meanwhile, considering the different system errors of different models and the aim for optimal improvement of AO, the different key regions for different models are selected (Region-3 above mentioned), all of which are also located in the midlatitudes of the North Pacific. Hereafter, the area-weighted areal mean DY_SSTs for Region-3 is labeled DY_SSTI. The DY_SSTIs indicate significant relationship with observed DY_AOI with correlation coefficients of 0.42, 0.41, 0.41, 0.39, and 0.37, all significant at the 99% confidence level (IFM is at 95% confidence level with 0.34) for the ECWMF, MF, UKMO, and CMCC models and the MME, respectively. In addition, the correlation coefficients between the time series of DY_SSTI derived from the observations and ENSEMBLES predictions are calculated to show the good performance of ENSEMBLES models for DY_SSTI predictions with values of 0.59, 0.54, 0.60, 0.66, 0.64, and 0.74 corresponding to the ECWMF, IFM, MF, UKMO, and CMCC models and the MME, respectively, beyond the 99% confidence level.

From observational analyses and numerical experiments, increased snow cover may lead to a negative phase of AO with wave-mean flow interactions (Gong et al., 2003; Saito & Cohen, 2003). It is suggested that enhanced autumn Eurasia snow cover increases the vertical wave energy propagation upward into the stratosphere, weakening the polar vortex, generating a negative winter AO pattern (Cohen et al., 2007). Therefore, the autumn snow cover may be a potential predictor for AO prediction.

However, the snow cover index (DY_SNCI: area-weighted areal mean DY of snow cover over East Asia; figure not shown) is non-independent with DY_SICI with a correlation coefficient of −0.24. It is revealed that the declining sea ice acts as moisture source and modulates atmospheric circulation, resulting in enhanced snow cover (Wegmann et al., 2015). For best improvement of AO prediction in ENSEMBLES, DY_SICI are selected to be the preceding predictor. The improved results of DY_SNCI and DY_SSTI are also shown in section 5.

### 4.2. The Dynamical-Statistical Model and Results

From above-mentioned analysis, two predictors, that is, DY_SICI and DY_SSTI, are used to establish a dynamical-statistical model (1) to improve the DJF AOI predicted by ENSEMBLES. According to the interannual increment approach, the improved DJF AOI is produced by adding the improved DY_AOI obtained from the dynamical-statistical model to the observed DJF AOI from the previous year.

These dynamical-statistical models are evaluated by two-year-out cross-validation for 1962−2006 and independent hindcasts for the hindcasting period 1990−2006. The results of the cross-validation are shown in Figure 7. It can be seen that the predicted DJF DY_AOI is largely improved in comparison to the direct outputs by ENSEMBLES, resulting in more consistency with the observed DJF DY_AOI (Figure 7a). The correlation coefficients of the DY_AOIs derived from the observations and from the improved results are 0.60, 0.57, 0.59, 0.60, 0.52, and 0.55 (Table 2), all at 99% significant confidence level for the ECWMF, IFM, MF, UKMO, CMCC models, and for the MME, respectively. These values are substantially higher than the raw model values (0.02, 0.31, 0.30, 0.31, −0.11, and 0.33, respectively). The corresponding RMSEs between the improved and observed DY_AOIs are reduced by 46%, 38%, 40%, 40%, 50%, and 37% (Table 2). These results indicate that the DY_AOI is best determined by the dynamical-statistical model for all the models of ENSEMBLES.

Figure 7b displays the improved AOIs obtained by adding the predicted DJF DY_AOI to the observed DJF AOI for the previous year. The time series of these improved AOIs for all models of ENSEMBLES are largely consistent with the time series of the observed DJF AOI. The corresponding correlation coefficients between the observed and improved time series are 0.54, 0.51, 0.54, 0.54, 0.48, and 0.51, all significant at the 99% confidence level for the ECWMF, IFM, MF, UKMO, CMCC, models and for the MME, respectively. These values indicate better predictions by the interannual increment approach for all models relative to the raw model

**Table 2**

*Correlation Coefficients Between the Observed and Predicted AOIs and DY_AOIs Based on the Cross-Validation of the Dynamical-Statistical Model for 1962–2006, Along With the RMSEs (Improvement of the RMSEs Is Shown in Parentheses and Is Relative to the Raw Model Outputs)*

| ENSEMBLES model | Correlation coefficients | | RMSE | |
|---|---|---|---|---|
| | AOI | DY_AOI | AOI | DY_AOI |
| ECWMF | 0.54** | 0.60** | 1.05 (17%) | 1.03 (46%) |
| IFM | 0.51** | 0.57** | 1.08 (9%) | 1.05 (38%) |
| MF | 0.54** | 0.59** | 1.06 (8%) | 1.04 (40%) |
| UKMO | 0.54** | 0.60** | 1.04 (16%) | 1.03 (40%) |
| CMCC | 0.48** | 0.52** | 1.13 (22%) | 1.09 (50%) |
| MME | 0.51** | 0.55** | 1.10 (3%) | 1.07 (37%) |

*Note.* "*" and "**" indicate statistical significance at the 95% and 99% confidence levels, respectively, based on Student's *t* test with effective degrees of freedom.

results (0.20, 0.29, 0.33, 0.22, −0.05, and 0.36). The percentage improvements in the RMSE of the AOI for the ECWMF, IFM, MF, UKMO, and CMCC models and the MME are 17%, 9%, 8%, 16%, 22%, and 3%, respectively. And the little improvement of RMSE of MME model may be because the reasonable AOI prediction of MME model. These results demonstrate the strong ability of the interannual increment approach to improve the AO predictions. However, there are several years where the improved AOI still displays a discrepancy with the observed AOI, including 1968, 1972, 1977, 1989, and 2001 (Figure 7b); these discrepancies are mainly due to the limitations of the DY_AOI predictions (Figure 7a). In addition, all of the improved AOIs for ENSEMBLES successfully captured the interdecadal variability of the observed AOIs, indicating a remarkable improvement relative to the direct predictions produced by ENSEMBLES (Figure 3a). Overall, the dynamical-statistical model combined with the interannual increment approach shows strong potential for improving the DJF AOI predictions of ENSEMBLES.

The results of independent hindcasts for the period 1990−2006 are shown in Figure 8. The time series of the predicted DY_AOIs are consistent with the time series of the observed DY_AOIs (Figure 8a) with correlation coefficients of 0.76, 0.73, 0.76, 0.72, 0.79, and 0.75, significant at 95%, 99%, 99%, 95%, 99%, and 99% confidence level for the ECWMF, IFM, MF, UKMO, CMCC models, and for the MME, respectively (Table 3). The different significance levels of similar values of the correlation coefficients are because the improved DY_AOI of all models have different effective degrees of freedom. These correlation coefficients are greatly improved in comparison with the values (0.26, 0.35, 0.40, 0.34, −0.08, and 0.39) of raw model predictions (Table 1). The corresponding RMSEs in independent hindcasts are reduced by 58%, 37%, 53%, 39%, 54%, and 42% (Table 3). These results again demonstrate the strong potential of the dynamical-statistical model to improve the DY_AOI. Meanwhile, the final predicted AOIs for the ECWMF, IFM, MF, UKMO, CMCC models, and for the MME are produced by an interannual increment approach; the predicted AOIs are consistent with the observed AOIs (Figure 8b). The correlation coefficients between the predicted and observed AOIs are 0.66, 0.62, 0.67, 0.65, 0.67, and 0.66, at 95%, 95%, 99%, 95%, 99%, and 99% significant confidence level for the ECWMF, IFM, MF, UKMO, CMCC models, and for the MME, respectively (Table 3). These values in hindcast are substantially higher than the corresponding raw model outputs for the period 1990−2006 (0.09, 0.08, 0.31, −0.07, 0.10, and 0.15; Table 1). The percentage improvements in the RMSEs for the hindcast are 41%, 26%, 35%, 31%, 30%, and 29%. Thus, the dynamical-statistical model and interannual increment approach can predict the DJF AO better than previous approaches. However, in several years, the hindcast results for all ENSEMBLES models have larger deviations relative to the observations; these years include 1994, 2001, and 2002 (Figure 8b), and the deviations are mainly due to the deviations of the DY_AOI predictions in hindcasts (Figure 8a). Therefore, the dynamical-statistical model has the ability to improve predictions of the interannual variability of the DJF AO, and it can be applied to all the ENSEMBLES models.

## 5. Discussion and Conclusions

This study evaluates the capability of ENSEMBLES models for winter AO predictions during 1962−2006. All of the ENSEMBLES models have a good predictive capability for predicting the SLP and can accurately present the spatial patterns and intensities of the winter SLP in the NH. The inconsistent performances of most ENSEMBLES models for winter AO predictions are noted. Specifically, all of the models can capture the zonally symmetric pattern of the AO, but they tend to overestimate the anomalies in the North Pacific and underestimate the anomalies in
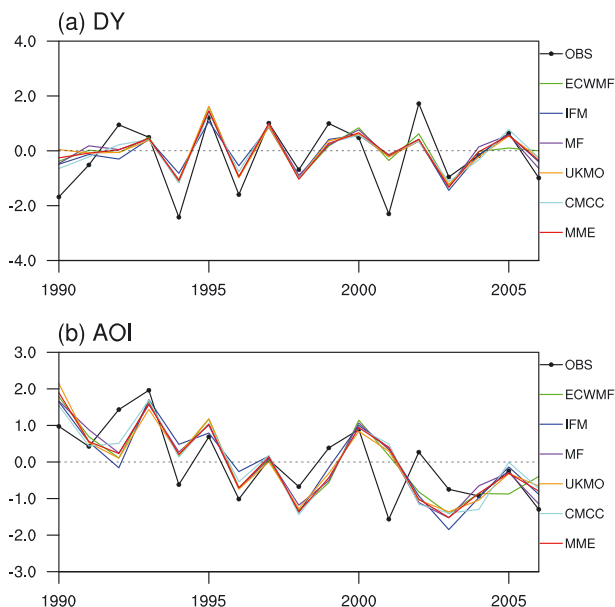


**Figure 8.** Predicted (a) DY of the AOI and (b) AOI during 1990–2006 for the observations, ECWMF, IFM, MF, UKMO, CMCC, and MME, in which the predicted DY uses the dynamical–statistical prediction model in the independent hindcast.

**Table 3**

*Correlation Coefficients Between the Observed and Predicted AOIs and DY_AOIs Based on the Dynamical-Statistical Model in Independent Hindcast for 1990–2006, Along With the RMSEs (Improvement of RMSEs Is Shown in Parentheses and Is Relative to Raw Model Outputs)*

| ENSEMBLES model | Correlation coefficients | | RMSE | |
|---|---|---|---|---|
| | AOI | DY_AOI | AOI | DY_AOI |
| ECWMF | 0.66* | 0.76* | 0.84 (41%) | 0.86 (58%) |
| IFM | 0.62* | 0.73** | 0.89 (26%) | 0.91 (37%) |
| MF | 0.67** | 0.76** | 0.84 (31%) | 0.86 (53%) |
| UKMO | 0.65* | 0.72* | 0.90 (35%) | 0.90 (39%) |
| CMCC | 0.67** | 0.79** | 0.81 (30%) | 0.84 (54%) |
| MME | 0.66** | 0.75** | 0.85 (29%) | 0.87 (42%) |

*Note.* "*" and "**" indicate statistical significance at the 95% and 99% confidence levels, respectively, based on Student's *t* test with effective degrees of freedom.

the Arctic and North Atlantic. The IFM, CMCC, and MME models fail to predict the positions and intensities of the AO pattern anomalies in the Arctic and North Atlantic. Moreover, inconsistent predictions of the AOI are also found in ENSEMBLES models; most of the model-predicted AOIs are inconsistent with the observed AOIs during 1962–2006, although the MF and MME-predicted AOI has a significant correlation of 0.33 and 0.36. The performance of ENSEMBLES in the prediction of the DY of the AOI shows similar predictive capabilities.

To improve the AOI prediction accuracy of ENSEMBLES, a dynamical-statistical model is established utilizing the interannual increment approach and two predictors, namely, the observed SIC for the preceding SON in the East Siberian Sea and the Beaufort Sea and the ENSEMBLES-predicted SST for the concurrent DJF over the midlatitudinal Pacific in the NH. The results of the two-year-out cross-validation indicate that the dynamical-statistical model can produce DY_AOI predictions that are much better than the raw ENSEMBLES predictions; a notably improved AOI is obtained via the dynamical-statistical model. The correlation coefficients of the AOIs (DY_AOIs) between the observations and the improved results are greatly improved relative to the raw model predictions, and the corresponding RMSEs are greatly reduced (Table 2). Furthermore, an independent hindcast for 1990−2006 is also applied to evaluate the dynamical-statistical model. The results show that the dynamical-statistical model is capable of improving the AOI (DY_AOI) predictions of ENSEMBLES (Table 3).

In addition, the preceding SON snow cover in Asia has also been used to be the preceding predictor for its significant effect on winter AO (Saito & Cohen, 2003). Because the SON snow cover is nonindependent with SON sea ice, SON snow cover and ENSEMBLES-predicted SST are also tried to be predictors to improve the AOI. All the improved correlation coefficients are less than the value of 0.42, significant at 99% confidence level. But the improvements of snow cover and ENSEMBLES-predicted SST are far from the results of sea ice and ENSEMBLES-predicted SST (Table 2), indicating that these two predictors of snow cover and SST have less predictive skill than the two of sea ice and SST. We also attempt to improve the AOI by the direct use of interannual increment approach. The improved AOIs are got by adding the observed AOIs of the preceding year to the DY_AOIs from the UKMO and MME models, which has reasonable performance in DY_AOI prediction. The correlation coefficients between predicted and observed AOIs are 0.32 and 0.35 for MF and UKMO, respectively, both at a 95% significant confidence level, thereby yielding less or no improvement than the dynamical-statistical model. The above efforts for AO prediction indicate that the efficiency of the dynamical-statistical model and interannual increment approach depends on the selection of predictor and the predictive ability of the models used in the DY prediction of AO.

Overall, the dynamical-statistical model combined with the interannual increment approach yields more accurate winter AO predictions than ENSEMBLES. The ability of the interannual increment approach to amplify signals of year-to-year variability applies to all variables and signals that have considerable interannual variability, especially quasi-biennial oscillation. Therefore, the interannual increment approach can be used to improve the prediction of many climate variables in East Asia, including the air pollution in China (Wang, 2018). Because this approach can take advantage from the previous observed signal of climate variables, it may be a new clue to apply the interannual increment approach into the prediction of extreme weather event, even the decadal prediction of climate variables. Moreover, it is feasible and worthwhile to combine the interannual increment approach with other modeling methods, such as deep learning.

Finally, although the ENSEMBLES models have generally favorable capabilities for SST prediction, they do not predict the significantly negative relationship between the observed winter AO and the concurrent SST over the high-latitudinal Pacific of the NH (Figures 5c and 5d), thereby limiting the ability of the dynamical-statistical model to improve AO predictions in ENSEMBLES. Furthermore, more recent databases of seasonal forecasts such as Climate Forecast System version 2, Met Office Global Seasonal Forecast System 5

(GloSea5), show some enhanced predictive skill in seasonal and year-to-year predictions (Maclachlan et al., 2014; Saha et al., 2014), which will be evaluated in the future work.

# References

Baldwin, M. P., & Dunkerton, T. J. (1999). Propagation of the Arctic Oscillation from the stratosphere to the troposphere. *Journal of Geophysical Research*, *104*(D24), 30,937–30,946. https://doi.org/10.1029/1999JD900445

Cohen, J., Barlow, M., Kushner, P. J., & Saito, K. (2007). Stratosphere–troposphere coupling and links with Eurasian land surface variability. *Journal of Climate*, *20*, 5335–5343. https://doi.org/10.1175/2007JCLI1725.1

Doblas-Reyes, F. J., Weisheimer, A., Déqué, M., & Keenlyside, N. (2009). Addressing model uncertainty in seasonal and annual dynamical ensemble forecasts. *Quarterly Journal of the Royal Meteorological Society*, *135*, 1538–1559. https://doi.org/10.1002/qj.464

Fan, K., Liu, Y., & Chen, H. P. (2012). Improving the prediction of the East Asian summer monsoon: New approaches. *Weather and Forecasting*, *27*, 1017–1030. https://doi.org/10.1175/WAF-D-11-00092.1

Fan, K., Tian, B. Q., & Wang, H. J. (2016). New approaches for the skillful prediction of the winter North Atlantic Oscillation based on coupled dynamic climate models. *International Journal of Climatology*, *36*, 82–94. https://doi.org/10.1002/joc.4330

Fan, K., & Wang, H. J. (2010). Seasonal prediction of summer temperature over Northeast China using a year-to-year incremental approach. *Journal of Meteorological Research*, *24*, 269–275.

Fan, K., Wang, H. J., & Choi, Y. J. (2008). A physically-based statistical forecast model for the middle-lower reaches of the Yangtze River Valley summer rainfall. *Chinese Science Bulletin*, *53*, 602–609. https://doi.org/10.1007/s11434-008-0083-1

Gong, D. Y., & Ho, C. H. (2003). Arctic Oscillation signals in the East Asian summer monsoon. *Journal of Geophysical Research*, *108*(D2), 4066. https://doi.org/10.1029/2002JD002193

Gong, D. Y., Mao, R., & Fan, Y. D. (2006). East Asian dust storm and weather disturbance: Possible links to the Arctic Oscillation. *International Journal of Climatology*, *26*(10), 1379–1396. https://doi.org/10.1002/joc.1324

Gong, D. Y., & Wang, S. W. (2003). Influence of Arctic Oscillation on winter climate over China. *Journal of Geographical Sciences*, *13*(2), 208–216. https://doi.org/10.1007/bf02837460

Gong, G., Entekhabi, D., & Cohen, J. (2003). Modeled Northern Hemisphere winter climate response to realistic Siberian snow anomalies. *Journal of Climate*, *16*(23), 3917–3931. https://doi.org/10.1175/1520-0442(2003)016<3917:MNHWCR>2.0.CO;2

Han, T. T., Wang, H. J., & Sun, J. Q. (2017). Strengthened relationship between the Antarctic Oscillation and ENSO after the mid-1990s during austral spring. *Advances in Atmospheric Sciences*, *34*(1), 54–65. https://doi.org/10.1007/s00376-016-6143-6

He, S. P., Gao, Y. Q., Li, F., Wang, H. J., & He, Y. C. (2017). Impact of Arctic Oscillation on the East Asian climate: A review. *Earth-Science Reviews*, *164*, 48–62. https://doi.org/10.1016/j.earscirev.2016.10.014

He, S. P., & Wang, H. J. (2013). Impact of the November/December Arctic Oscillation on the following January temperature in East Asia. *Journal of Geophysical Research: Atmospheres*, *118*, 12,981–12,998. https://doi.org/10.1002/2013JD020525

He, S. P., & Wang, H. J. (2016). Linkage between the East Asian January temperature extremes and the preceding Arctic Oscillation. *International Journal of Climatology*, *36*(2), 1026–1032. https://doi.org/10.1002/joc.4399

He, S. P., Wang, H. J., Gao, Y. Q., & Li, F. (2019). Recent intensified impact of December Arctic Oscillation on subsequent January temperature in Eurasia and North Africa. *Climate Dynamics*, *52*(1-2), 1077–1094. https://doi.org/10.1007/s00382-018-4182-7

Huang, Y. Y., Wang, H. J., & Fan, K. (2014). Improving the prediction of the summer Asian–Pacific Oscillation using the interannual increment approach. *Journal of Climate*, *27*(21), 8126–8134. https://doi.org/10.1175/JCLI-D-14-00209.1

Kalnay, E., Kanamitsu, M., Kistler, R., Collins, W. G., Deaven, D., Gandin, L., et al. (1996). The NCEP/NCAR 40-year reanalysis project. *Bulletin of the American Meteorological Society*, *77*(3), 437–471. https://doi.org/10.1175/1520-0477(1996)077<0437:TNYRP>2.0.CO;2

Kang, D., Lee, M., Im, J., Kim, D., Kim, H. M., Kang, H. S., et al. (2014). Prediction of the Arctic Oscillation in boreal winter by dynamical seasonal forecasting systems. *Geophysical Research Letters*, *41*, 3577–3585. https://doi.org/10.1002/2014GL060011

Kim, B. M., Son, S. W., Min, S. K., Jeong, J. H., Kim, S. J., Zhang, X. D., et al. (2014). Weakening of the stratospheric polar vortex by Arctic sea-ice loss. *Nature Communications*, *5*(1), 4646. https://doi.org/10.1038/ncomms5646

Li, C. F., Lu, R. Y., & Dong, B. W. (2012). Predictability of the western North Pacific summer climate demonstrated by the coupled models of ENSEMBLES. *Climate Dynamics*, *39*(1-2), 329–346. https://doi.org/10.1007/s00382-011-1274-z

Li, F., Wang, H. J., & Gao, Y. Q. (2014). On the strengthened relationship between the East Asian winter monsoon and Arctic oscillation: A comparison of 1950–70 and 1983–2012. *Journal of Climate*, *27*(13), 5075–5091. https://doi.org/10.1175/JCLI-D-13-00335.1

Li, F., Wang, H. J., & Gao, Y. Q. (2015). Extratropical ocean warming and winter Arctic sea ice cover since the 1990s. *Journal of Climate*, *28*(14), 5510–5522. https://doi.org/10.1175/JCLI-D-14-00629.1

Li, H. X., Chen, H. P., & Wang, H. J. (2017). Influence of North Pacific SST on heavy precipitation events in autumn over North China. *Atmospheric and Oceanic Science Letters*, *10*(1), 21–28. https://doi.org/10.1080/16742834.2017.1237256

Li, S., He, S. P., Li, F., & Wang, H. J. (2018). Simulated and projected relationship between the East Asian winter monsoon and winter Arctic Oscillation in CMIP5 models. *Atmospheric and Oceanic Science Letters*, *11*, 417–424. https://doi.org/10.1080/16742834.2018.1512356

Lin, Z. D., & Li, F. (2018). Impact of interannual variations of spring sea ice in the Barents Sea on East Asian rainfall in June. *Atmospheric and Oceanic Science Letters*, *11*, 275–281. https://doi.org/10.1080/16742834.2018.1454249

Liu, J. P., Curry, J. A., Wang, H. J., Song, M., & Horton, R. M. (2012). Impact of declining Arctic sea ice on winter snowfall. *Proceedings of the National Academy of Sciences*, *109*, 4074–4079. https://doi.org/10.1073/pnas.1114910109

Livezey, R. E., & Chen, W. Y. (1983). Statistical field significance and its determination by Monte Carlo techniques. *Monthly Weather Review*, *111*(1), 46–59. https://doi.org/10.1175/1520-0493(1983)111<0046:SFSAID>2.0.CO;2

Maclachlan, C., Arribas, A., Peterson, K. A., & Maidens, A. (2014). Global Seasonal forecast system version 5 (GloSea5): A high-resolution seasonal forecast system. *Quarterly Journal of the Royal Meteorological Society*, *141*(689), 1072–1084. https://doi.org/10.1002/qj.2396

Mao, R., Gong, D. Y., Bao, J. D., & Fan, Y. D. (2011). Possible influence of Arctic Oscillation on dust storm frequency in North China. *Journal of Geographical Sciences*, *21*, 207–218. https://doi.org/10.1007/s11442-011-0839-4

Marshall, J., Kushnir, Y., Battisti, D., Chang, P., Czaja, A., Dickson, R., et al. (2001). North Atlantic climate variability: Phenomena, impacts and mechanisms. *International Journal of Climatology*, *21*(15), 1863–1898. https://doi.org/10.1002/joc.693

Michaelsen, J. (1987). Cross-validation in statistical climate forecast models. *Journal of Climate and Applied Meteorology*, *26*(11), 1589–1600. https://doi.org/10.1175/1520-0450(1987)026<1589:CVISCF>2.0.CO;2

Mitchell, D. M., Gray, L. J., Anstey, J., Baldwin, M. P., & Charlton-Perez, A. J. (2013). The influence of stratospheric vortex displacements and splits on surface climate. *Journal of Climate*, *26*, 2668–2682. https://doi.org/10.1175/JCLI-D-12-00030.1

Qian, C., Zhou, W., Yang, X. Q., & Chan, J. C. L. (2018). Statistical prediction of non-Gaussian climate extremes in urban areas based on the first-order difference method. *International Journal of Climatology*, 38, 2889–2898. https://doi.org/10.1002/joc.5464

Qian, Z. L., Wang, H. J., & Sun, J. Q. (2011). The hindcast of winter and spring Arctic and Antarctic Oscillation with the coupled climate models. *Journal of Meteorological Research*, 25, 340–354. https://doi.org/10.1007/s13351-011-0309-z

Rayner, N. A., Parker, D. E., Horton, E. B., Folland, C. K., Alexander, L., Rowell, D. P., et al. (2003). Global analyses of sea surface temperature, sea ice, and night marine air temperature since the late nineteenth century. *Journal of Geographical Sciences*, 108(D14), 4407. https://doi.org/10.1029/2002JD002670

Riddle, E. E., Butler, A. H., Furtado, J. C., Cohen, J. L., & Kumar, A. (2013). CFSv2 ensemble prediction of the wintertime Arctic Oscillation. *Climate Dynamics*, 41, 1099–1116. https://doi.org/10.1007/s00382-013-1850-5

Saha, S., Moorthi, S., Wu, X. R., Wang, J. D., Nadiga, S., Tripp, P., et al. (2014). The NCEP Climate Forecast System version 2. *Journal of Climate*, 27, 2185–2208. https://doi.org/10.1175/JCLI-D-12-00823.1

Saito, K., & Cohen, J. (2003). The potential role of snow cover in forcing interannual variability of the major Northern Hemisphere mode. *Geophysical Research Letters*, 30(6), 1302. https://doi.org/10.1029/2002GL016341

Smith, T. M., Reynolds, R. W., Peterson, T. C., & Lawrimore, J. (2008). Improvements to NOAA's historical merged land–ocean surface temperature analysis (1880–2006). *Journal of Climate*, 21, 2283–2296. https://doi.org/10.1175/2007JCLI2100.1

Stammerjohn, S. E., & Smith, R. C. (1997). Opposing Southern Ocean climate patterns as revealed by trends in regional sea ice coverage. *Climatic Change*, 37(4), 617–639. https://doi.org/10.1023/A:1005331731034

Sun, B., & Wang, H. J. (2013). Larger variability, better predictability? *International Journal of Climatology*, 33, 2341–2351. https://doi.org/10.1002/joc.3582

Thompson, D. W. J., & Wallace, J. M. (1998). The Arctic Oscillation signature in the wintertime geopotential height and temperature fields. *Geophysical Research Letters*, 25(9), 1297–1300. https://doi.org/10.1029/98GL00950

Thompson, D. W. J., & Wallace, J. M. (2000). Annular modes in the extratropical circulation. Part I: Month-to-month variability*. *Journal of Climate*, 13(5), 1018–1036. https://doi.org/10.1175/1520-0442(2000)013<1018:AMITEC>2.0.CO;2

Thompson, D. W. J., & Wallace, J. M. (2001). Regional climate impacts of the Northern Hemisphere annular mode. *Science*, 293(5527), 85–89. https://doi.org/10.1126/science.1058958

Tian, B. Q., & Fan, K. (2015). A skillful prediction model for winter NAO based on Atlantic sea surface temperature and Eurasian snow cover. *Weather and Forecasting*, 30, 197–205. https://doi.org/10.1175/WAF-D-14-00100.1

Tian, B. Q., Fan, K., & Yang, H. Q. (2018). East Asian winter monsoon forecasting schemes based on the NCEP's climate forecast system. *Climate Dynamics*, 51, 2793–2805. https://doi.org/10.1007/s00382-017-4045-7

Wang, H. J. (2018). On assessing haze attribution and control measures in China. *Atmospheric and Oceanic Science Letters*, 11(2), 120–122. https://doi.org/10.1080/16742834.2018.1409067

Wegmann, M., Orsolini, Y., Vázquez, M., Gimeno, L., Nieto, R., Bulygina, O., et al. (2015). Arctic moisture source for Eurasian snow cover variations in autumn. *Environmental Research Letters*, 10, 054015. https://doi.org/10.1088/1748-9326/10/5/054015

Weisheimer, A., Doblas-Reyes, F. J., Palmer, T. N., Alessandri, A., Arribas, A., Déqué, M., et al. (2009). ENSEMBLES: A new multi-model ensemble for seasonal-to-annual predictions—Skill and progress beyond DEMETER in forecasting tropical Pacific SSTs. *Geophysical Research Letters*, 36, L21711. https://doi.org/10.1029/2009GL040896

Wettstein, J. J., & Mearns, L. O. (2002). The influence of the North Atlantic–Arctic Oscillation on mean, variance, and extremes of temperature in the northeastern United States and Canada. *Journal of Climate*, 15(24), 3586–3600. https://doi.org/10.1175/1520-0442(2002)015<3586:TIOTNA>2.0.CO;2

Xu, X. P., He, S. P., Li, F., & Wang, H. J. (2018). Impact of northern Eurasian snow cover in autumn on the warm Arctic–cold Eurasia pattern during the following January and its linkage to stationary planetary waves. *Climate Dynamics*, 50(5-6), 1993–2006. https://doi.org/10.1007/s00382-017-3732-8

Xu, X. P., Li, F., He, S. P., & Wang, H. J. (2018). Subseasonal reversal of East Asian surface temperature variability in winter 2014/15. *Advances in Atmospheric Sciences*, 35(6), 737–752. https://doi.org/10.1007/s00376-017-7059-5

Yang, S. H., & Lu, R. Y. (2014). Predictability of the East Asian winter monsoon indices by the coupled models of ENSEMBLES. *Advances in Atmospheric Sciences*, 31(6), 1279–1292. https://doi.org/10.1007/s00376-014-4020-8

Yin, Z. C., & Wang, H. J. (2016). Seasonal prediction of winter haze days in the north central North China Plain. *Atmospheric Chemistry and Physics*, 16(23), 14,843–14,852. https://doi.org/10.5194/acp-16-14843-2016

Zhang, D. P., Huang, Y. Y., Sun, B., Li, F., & Wang, H. J. (2019). Verification and improvement of the ability of CFSv2 to predict the Antarctic Oscillation in boreal spring. *Advances in Atmospheric Sciences*, 36(3), 292–302. https://doi.org/10.1007/s00376-018-8106-6

Zhao, L. N., Ma, Q. Y., Yang, G. M., Wang, X. R., Zhao, L. Q., Yang, X. D., et al. (2008). Disasters and its impact of a severe snow storm and freezing rain over southern China in January 2008. *Climatic and Environmental Research* (in Chinese, 13(4), 556–566. https://doi.org/10.3878/j.issn.1006-9585.2008.04.20

Zhu, Y. L., Wang, H. J., Wang, T., & Guo, D. (2018). Extreme spring cold spells in North China during 1961–2014 and the evolving processes. *Atmospheric and Oceanic Science Letters*, 11(5), 432–437. https://doi.org/10.1080/16742834.2018.1514937